6436 *Inorg. Chem.* **2010**, *49*, 6436–6442
DOI: 10.1021/ic100021f

Inorganic Chemistry
Article

A Unique Cobalt(II)-Based Molecular Magnet Constructed of Hydroxyl/Carboxylate Bridges with a 3D Pillared-Layer Motif

Ming-Hua Zeng,*,[†,‡] Yan-Ling Zhou,[†,‡] Mei-Chun Wu,[†,‡] Hao-Ling Sun,*,[§] and Miao Du*,[⊥]

[†] *Key Laboratory of Synthetic and Natural Functional Molecule Chemistry of the Ministry of Education, Northwest University, Xi'an 710069, People's Republic of China,* [‡] *School of Chemistry and Chemical Engineering, Guangxi Normal University, Guilin 541004, People's Republic of China,* [§] *Department of Chemistry, Beijing Normal University, Beijing 100875, People's Republic of China, and* [⊥] *College of Chemistry and Life Science, Tianjin Normal University, Tianjin 300387, People's Republic of China*

Received January 5, 2010

A new pillared-layer coordination polymer, $[\mathrm{Co_3(pybz)_2(pico)_2}]_n$ (**1**; pybz = 4-(pyridin-4-yl)benzoate, pico = 3-hydroxypicolinate), contains rare 2D $[\mathrm{Co_3(pico)_2}]_n^{2n+}$ layers formed by linear cobalt(II) trimers through the unusual μ_4-κN, O:κO′-μ_2:κO″-μ_2 bridging mode of pico ligands, which are further cross-pillared by exotridentate bridging pybz ligands to form a three-dimensional structure with an unusual uninodal 8-connected body-centered-cubic topology. The bulk magnetic behavior of **1** exhibits ferrimagnetic long-range ordering below 2.6 K, which mainly arises from the cooperative magnetic effect of the intra- and intertrimer arrangements in the 2D magnetic system based on the nature of the exchange modes of μ_2-hydroxyl, μ_2-carboxylate oxygen, and 1,1,3-μ_3-carboxylate bridges.

Introduction

In molecular magnetism, magnetic coordination polymers provide good examples to better understand some fundamental phenomena and their correlation (e.g., ferromagnetic, antiferromagnetic, ferrimagnetic, spin canting, metamagnetic transition, spin−flip transition, etc.).[1] Among them, only a few ferromagnets exhibiting long-range ordering have been synthesized because of the fact that ferromagnetic coupling is usually weaker compared with the antiferromagnetic one.[1] In particular, magnetic couplers that can transmit ferromagnetic coupling are relatively rare, and until now, few hetero/homometallic ferromagnets constructed by a cyano[2] or an azide[3] bridge have been documented in which a uniform magnetic exchange pathway governs throughout the whole structure.[4] Conventional ferrimagnetic systems of metal complexes (i.e., heterospin systems contain two different magnetic ions with nearest-neighbor antiferromagnetic exchange coupling) are well represented by numerous compounds whose metal atoms are bridged through, for example, cyanide or oxalate groups.[1−3] Unfortunately, only a few homospin homometallic systems are known that exhibit long-range ferrimagnetic order, with the reason for such a scarcity being linked to the necessity for noncompensation moments, such as a specific alternation of ferromagnetic (F) and antiferromagnetic (AF) interactions.[1,5] Besides cyano or azido, the carboxylate group has also been widely used in the synthesis of coordination polymers. However, only quite limited carboxylate-bridged ferromagnetic or ferrimagnetic systems are known.[5] Moreover, the carboxylate group shows versatile coordination characteristics and/or bridging modes, and the types of magnetic interactions can also be very

---

*To whom correspondence should be addressed. E-mail: zmh@mailbox.gxnu.edu.cn (M.-H.Z.), haolingsun@bnu.edu.cn (H.-L.S.), dumiao@public.tpt.tj.cn (M.D.).

(1) (a) Kahn, O. *Molecular Magnetism*; VCH Publishers: New York, 1993. (b) Miller, J. S.; Drillon, M. *Magnetism: Molecules to Materials I-V*; Wiley-VCH Publishers: Weinheim, Germany, 2001. (c) Laget, V.; Hornick, C.; Rabu, P.; Drillon, M.; Ziessel, R. *Coord. Chem. Rev.* **1998**, *178−180*, 1533 and references cited therein.

(2) For example, see: (a) Dunbar, K. R.; Heintz, R. A. *Prog. Inorg. Chem.* **1997**, *54*, 118 and references cited therein. (b) Verdaguer, M.; Bleuzen, A.; Marvaud, V.; Vaissermann, J.; Seuleiman, M.; Desplanches, C.; Scuiller, A.; Train, C.; Garde, R.; Gelly, G.; Lomenech, C.; Rosenman, I.; Veillet, P.; Cartier, C.; Villain, F. *Coord. Chem. Rev.* **1999**, *190*, 1023 and references cited therein. (c) Ohba, M.; Ōkawa, H. *Coord. Chem. Rev.* **2000**, *198*, 313 and references cited therein. (d) Przychodzén, P.; Korzeniak, T.; Podgajny, R.; Sieklucka, B. *Coord. Chem. Rev.* **2006**, *250*, 2234 and references cited therein.

(3) For example, see: (a) Ribas, J.; Escuer, A.; Monfort, M.; Vicente, R.; Cortes, R.; Lezama, L.; Rojo, T. *Coord. Chem. Rev.* **1999**, *193−195*, 1027 and references cited therein. (b) Wang, X. Y.; Wang, Z. M.; Gao, S. *Chem. Commun.* **2008**, 281 and references cited therein. (c) Zeng, Y. F.; Hu, X.; Liu, F. C.; Bu, X. H. *Chem. Soc. Re.v* **2009**, *38*, 469 and references cited therein. (d) Sun, H. L.; Wang, Z. M.; Gao, S. *Chem.—Eur. J.* **2009**, *15*, 1757.

(4) (a) Gu, Z. G.; Song, Y.; Zuo, J. L.; You, X. Z. *Inorg. Chem.* **2007**, *46*, 9522. (b) Shen, Z.; Zuo, J. L.; Gao, S.; Song, Y.; Che, C. M.; Fun, H. K.; You, X. Z. *Angew. Chem., Int. Ed.* **2000**, *39*, 3633.

(5) (a) Kurmoo, M. *Chem. Soc. Rev.* **2009**, *38*, 1353 and references cited therein. (b) Kurmoo, M.; Kumagai, H.; Chapman, K. W.; Kepert, C. J. *Chem. Commun.* **2005**, 3012. (c) Snejko, N.; Gutirrez-Puebla, E.; Martnez, J. L.; Monge, M. A.; Ruiz-Valero, C. *Chem. Mater.* **2002**, *14*, 1879. (d) Biswas, C.; Mukherjee, P.; Drew, M. G. B.; Gómez-García, C. J.; Clemente-Juan, J. M.; Ghosh, A. *Inorg. Chem.* **2007**, *46*, 10771.

Scheme 1. Coordination Modes of pico

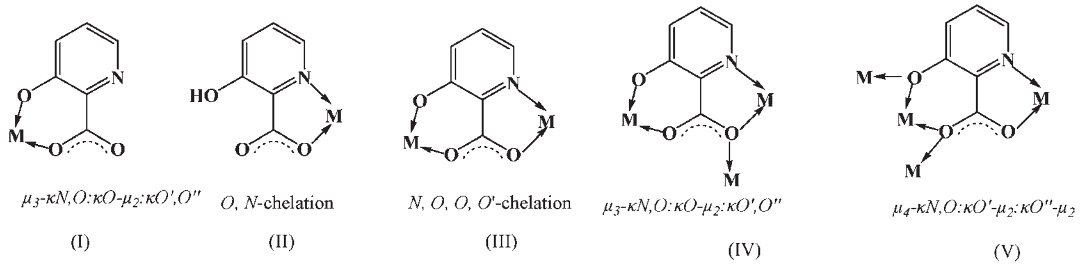

diverse with a slight change of the environments of the metal centers,[6] which are the obstacles in the synthesis of carboxylate-bridged complexes with predictable ferromagnetic or ferrimagnetic coupling in the whole three-dimensional (3D) structure assembly. In fact, among the various bridging modes, anti−anti and syn−syn configurations are most likely to transmit strong antiferromagnetic interactions,[7] whereas weak ferromagnetic couplings occur in most cases of the syn−anti mode and less-common 1,1,3-μ_3- and rare 1,1-μ_2-bridging modes.[8] Recent references show that the relationship between the carboxylate coordination mode and the sign of coupling is not simple, which may depend on several parameters including the metal ions (Cu, Ni, Co, Mn, etc.), the parallel situation of the axes of the coordination octahedron, and the completely parallel situation of spin orientation.[5a,7,8] Obviously, the design of high-dimensional metal carboxylates containing diverse superexchange bridges with predictable magnetic properties is still a challenge in the field of molecular magnetism. On the other hand, the research on cluster-based coordination polymers has attracted considerable attention for their intriguing architectures.[5a,6] Notably, most of them are obtained by oxo-centered metal clusters with carboxylate and/or pyridyl ligands, which still represent a chance for the above challenge in magnetochemistry.[6] Very recently, Natarajan, Drillon, and co-workers have reported a unique body-centered-cubic network of $[Co_4]$ magnetic clusters that shows interesting quasi-two-dimensional *XY* magnetic properties and slow relaxation.[9] Obviously, the long-range magnetic ordering is a consequence of magnetic coupling within the 3D structure, together with the magnetic anisotropy of spin carriers.[1] In addition, complicated magnetic anisotropy also has a significant influence on the bulky magnetism.[9,10]

In our previous work, we have reported two cobalt(II) metamagnets constructed of a 3-hydroxypicolinate (pico) ligand and a coligand of 4,4′-bipyridine or isonicotinate.[10] $[Co_4(pico)_4(4,4'\text{-bpy})_3(H_2O)_2]_n \cdot 2nH_2O$ shows a rare 3D interpenetrating framework, in which the Co^{II} ions are linked by the pico ligands using a μ_2-κN,O:κO′,O″ mode, which transmits antiferromagnetic coupling,[10a] while $[Co_3(ina)_2(pico)_2(H_2O)_2]_n$ displays a unique 3D pillared-layer motif, in which pico adopts a μ_3-κN,O:κO-μ_2:κO′,O″ bridging mode and also transmits antiferromagnetic coupling.[10b] Such a pico ligand having a hydroxyl group in the pyridyl-type carboxylate provides an additional coordination site and allows the formation of five- and six-membered chelated rings, which can stabilize the resulting solid networks (Scheme 1).[11] Encouraged by our previous result that pico is an efficient magnetic coupler, we have also chosen the pico ligand and introduced another longer ditopic coligand of pyridine−benzenecarboxylic acid (pybz) to replace 4,4′-bpy or isonicotinate. We hope to use this long coligand to weaken the interlayer antiferromagnetic coupling of $[Co_3(ina)_2(pico)_2(H_2O)_2]_n$ to get a novel complicated network with predictable ferromagnetic or ferrimagnetic long-range ordering. Herein, we describe the synthesis, structural analysis, and magnetic studies of a quite unusual homospin ferrimagnet $[Co_3(pybz)_2(pico)_2]_n$, which shows a unique 3D pillared-layer motif that is constructed of pico and a long coligand of pybz.

Experimental Section

Materials and Physical Measurements. All chemicals were commercially available and used as received without further purification. The C, H, and N microanalyses were carried out with an Elemental Vario-EL CHNS elemental analyzer. The FT-IR spectra were recorded from KBr pellets in the range of 4000−400 cm^{-1} on a Bio-Rad FTS-7 spectrometer. Temperature- and field-dependent magnetic measurements were carried out on a SQUID-MPMS-XL-7 magnetometer. Diamagnetic corrections were made with Pascal's constants.[12]

Synthesis. Complex **1** was prepared from a mixture of H_2-pico (0.139 g, 1 mmol) in an aqueous solution (6 mL) of NaOH

---

(6) (a) Rao, C. N. R.; Natarajan, S.; Vaidhyanathan, R. *Angew. Chem., Int. Ed.* **2004**, *43*, 1466. (b) Janiak, C. *Dalton Trans.* **2003**, 2781. (c) Batten, S. R.; Neville, S. M.; Turner, D. R. *Coordination Polymers Design, Analysis and Application*; The Royal Society of Chemistry: London, 2009.

(7) (a) Zheng, Y. Z.; Xue, W.; Tong, M. L.; Chen, X. M.; Grandjean, F.; Long, G. J. *Inorg. Chem.* **2008**, *47*, 4077. (b) Chen, X. N.; Xue, W.; Zhang, W. X.; Chen, X. M. *Chem. Mater.* **2008**, *20*, 5345. (c) Kostakis, G. E.; Mondal, K. C.; Abbas, G.; Lan, Y. H.; Novitchi, G.; Buth, G.; Anson, C. E.; Powell, A. K. *CrystEngComm* **2009**, *11*, 2084. (d) Kampert, E.; Janssen, F. F. B. J.; Boukhvalov, D. W.; Russcher, J. C.; Smits, J. M. M.; de Gelder, R.; de Bruin, B.; Christianen, P. C. M.; Zeitler, U.; Katsnelson, M. I.; Maan, J. C.; Rowan, A. E. *Inorg. Chem.* **2009**, *48*, 11903.

(8) (a) Wang, X. Y.; Sevov, S. C. *Inorg. Chem.* **2008**, *47*, 1037. (b) Wang, X. Y.; Wang, L.; Wang, Z. M.; Su, G.; Gao, S. *Chem. Mater.* **2005**, *17*, 6369. (c) Arora, H.; Lloret, F.; Mukherjee, R. *Inorg. Chem.* **2009**, *48*, 1158. (d) Arora, H.; Lloret, F.; Mukherjee, R. *Dalton Trans.* **2009**, 9759. (e) Beghidja, A.; Rogez, G.; Rabu, P.; Welter, R.; Drillon, M. *J. Mater. Chem.* **2006**, *16*, 2715.

(9) Mahata, P.; Natarajan, S.; Panissod, P.; Drillon, M. *J. Am. Chem. Soc.* **2009**, *131*, 10140.

(10) (a) Zeng, M. H.; Zhang, W. X.; Sun, X. Z.; Chen, X. M. *Angew. Chem., Int. Ed.* **2005**, *44*, 3079. (b) Zhou, Y. L.; Wu, M. C.; Zeng, M. H.; Liang., H. *Inorg. Chem.* **2009**, *48*, 10146. (c) Yao, M. X.; Zeng, M. H.; Zou, H. H.; Zhou, Y. L.; Liang, H. *Dalton Trans.* **2008**, 2428. (d) Zeng, M. H.; Feng, X. L.; Zhang, W. X.; Chen., X.-M. *Dalton Trans.* **2006**, 5294. (e) Zeng, M. H.; Wu, M. C.; Liang, H.; Zhou, Y. L.; Chen, X.-M.; Ng, S. W. *Inorg. Chem.* **2007**, *46*, 7241. (f) Zeng, M. H.; Wang, B.; Wang, X. Y.; Zhang, W. X.; Chen, X. M.; Gao, S. *Inorg. Chem.* **2006**, *45*, 7069.

(11) (a) Quintal, S. M. O.; Nogueira, H. I. S.; Carapuca, H. M.; Felix, V.; Drew, M. G. B. *J. Chem. Soc., Dalton Trans.* **2001**, 3196. (b) Casny, M.; Rehder, D. *Dalton Trans.* **2004**, 839. (c) Soares-Santos, P. C. R.; Nogueira, H. I. S.; Felix, V.; Drew, M. G.; Ferreira, B. R. A. S.; Carlos, L. D.; Trindade, T. *Chem. Mater.* **2003**, *15*, 100. (d) Popović, Z.; Pavlović, G.; Vinković, M.; Vikić-Topić, D.; Linarić, M. R. *Polyhedron* **2006**, *25*, 2353. (e) Nakai, M.; Sekiguchi, F.; Obata, M.; Ohtsuki, C.; Adachi, Y.; Sakurai, H.; Orvig, C.; Rehder, D.; Yano, S. *J. Inorg. Biochem.* **2005**, *99*, 1275.

(12) Boudreaux, E. A.; Mulay, J. N. *Theory and Application of Molecular Diamagnetism*; John Wiley and Sons: New York, 1976.

Table 1. Summary of the Crystallographic Data for **1**

compound	**1**
empirical formula	$C_{36}H_{22}Co_3N_4O_{10}$
fw	847.39
cryst syst	monoclinic
space group	$P2_1/c$
a/Å	12.568(1)
b/Å	13.419(1)
c/Å	10.625(1)
β/deg	97.005(2)
V/Å^3	1778.5(3)
Z	2
D_c/g cm^{-3}	1.582
abs coeff (mm^{-1})	1.446
F(000)	854
reflns collected, independent	3484, 3123
max/min transmn	0.8571/0.7808
R1/wR2 [$I > 2\sigma(I)$]	0.0428/0.1018
GOF on F^2	1.138

Table 2. Selected Bond Lengths (Å) and Angles (deg) for **1**

Co1−O2	2.035(2)	Co1−O3−Co2	93.17(9)	O1−Co2−O3	91.47(9)
Co1−O3	2.219(2)	Co1−O4−Co2	95.85(9)	O1−Co2−O4	87.59(9)
Co1−O5b	2.075(2)	O2−Co1−N2b	82.22(1)	O1−Co2−O1c	180.0(2)
Co1−N2b	2.125(3)	O2−Co1−O4c	92.27(1)	O1−Co2−O3c	88.53(9)
Co1−O4c	2.124(2)	O2−Co1−N1e	172.90(1)	O1−Co2−O4c	92.41(9)
Co1−N1e	2.100(3)	O3−Co1−O5a	105.74(9)	O3−Co2−O4	93.15(9)
Co2−O1	2.199(2)	O3−Co1−N2b	166.05(1)	O1c−Co2-O3	88.53(9)
Co2−O3	1.997(2)	O3−Co1−O4c	78.58(8)	O3−Co1−N1e	93.89(1)
Co2−O4	2.005(2)				

(0.080 g, 2 mmol) and pybz (0.092 g, 0.75 mmol) in EtOH (2 mL), which was then added to an aqueous solution (2 mL) of $Co(NO_3)_2 \cdot 6H_2O$ (0.291 g, 1 mmol). The mixture was placed in a 23-mL Teflon-lined autoclave and heated at 150 °C for 48 h. The autoclave was cooled to room temperature at a rate of 10 °C h^{-1}, and red crystals of **1** were collected by filtration, washed with water, and dried in air (final yield: 66% based on cobalt). Elem anal. Calcd for **1**: C, 51.03; H, 2.62; N, 6.61. Found: C, 51.78; H, 2.54; N, 6.50. IR data (cm^{-1}; see Figure S1 in the Supporting Information): 3402 m, 1590 vs, 1562 s, 1461 s, 1397 vs, 1329 m, 1243 m, 1222 m, 1138 m, 1121 m, 761 m, 706 m, 509 m. We may conclude that a sharp peak at around 3402 cm^{-1} can be attributed to the μ_2-OH$^-$ group. No broad feature in the range of 3000−3800 cm^{-1} was observed, indicating the absence of water molecules in the title compound. The very strong peak at 1397 cm^{-1} corresponds to ν_{sym} of the chelating carboxylate group. The presence of very strong absorption bands around 1590 cm^{-1} confirms the fully deprotonated, coordinating carboxyl groups of the ligands pybz and pico, as revealed by the single-crystal structure analysis.

Crystal Structure Determination. Diffraction intensities for **1** were collected on a Bruker Smart Apex-II CCD diffractometer equipped with graphite-monochromated Mo Kα radiation (λ = 0.710 73 Å) at 173 K, using the $\omega-\theta$ scan mode in the range of 1.57° ≤ θ ≤ 25.10°. Raw frame data were integrated with the *SAINT* program. The structure was solved by direct methods using *SHELXTL* and refined by full-matrix least squares on F^2 using *SHELXTL*.[13] An empirical absorption correction was applied with the program *SADABS*. All non-hydrogen atoms were refined anisotropically. The crystallographic details are provided in Table 1, and the selected bond distances and angles are listed in Table 2. The CCDC number is 757661 for **1**.

Results and Discussion

Crystal Structure. Single-crystal X-ray structure determination reveals that **1** features a pillared-layer 3D motif, in which the 2D layers bridged by pico ligands are further connected via long pybz pillars (Figure 1). Within the 3D structure, two crystallographically independent Co^{II} ions (namely, Co1 and Co2) with octahedral coordination environments are found. The Co1 atom is coordinated by three oxygen atoms and one nitrogen atom from three pico ligands at equatorial positions and one oxygen atom and one nitrogen atom of two pybz ligands at axial sites [Co1−O = 2.035(2)−2.219(2) Å; Co1−N = 2.100(3)−2.125(3) Å]. The Co2 ion is coordinated, however, by four oxygen atoms (two carboxylate and two hydroxyl oxygen atoms) of two pico ligands at equatorial sites and two carboxylate oxygen atoms of pybz at axial sites [Co−O = 1.997(2)−2.199(2) Å]. Each Co2 atom is connected to two Co1 atoms through mixed bridges of μ_2-hydroxyl and μ_2-carboxylate oxygen atoms from pico ligands and two *syn*, *syn*-1,3-carboxylates from pybz ligands to form a linear trimer, with an intratrimer Co···Co separation of 3.066 Å. The Co1−O−Co2 angles are 93.17° and 95.85° for μ_2-hydroxyl and μ_2-carboxylate oxygen bridges, respectively. The Co···Co separation is shorter than those found in the reported oxo-bridged linear Co^{II} trimers.[6b,14] In this structure, each trimer is linked to four adjacent trimers by four pico ligands using μ_4-κN,O:κO′-μ_2:κO″-μ_2 bridging mode (Scheme 1, mode V), resulting in 2D $[Co_3(pico)_2]_n^{2n+}$ layers with the intertrimer Co···Co distance of 5.511 Å (Figure 2).

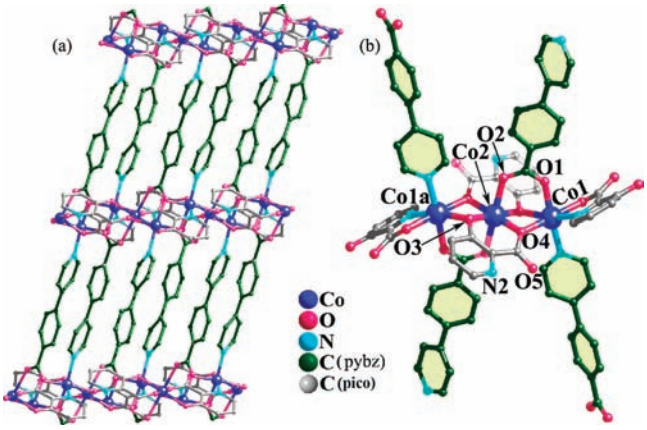

Figure 1. (a) Plot of a 3D pillared-layer structure of **1** viewed along the *b* axis. (b) Plot of the cobalt(II) coordination environments showing the pico bridges within the trimer in **1**. All hydrogen atoms are omitted for clarity.

The unique layers in **1** are cross-pillared by μ_3-pybz ligands with an exotridentate bridging mode to form a 3D structure with an interlayer Co···Co distance of ca. 12.4 Å. The pybz pillars of **1** with twisting (the torsion angles of the fragments of C7−O4−O5−Co2 and C7−O4−O5−Co1 are 168.60° and 161.59°, respectively) are a result of orientation adjustment to achieve the stable coordination geometries for Co^{II} ions from the adjacent layers. Hence, the closely packed and tilting pybz pillars within **1** are too compact to provide voids for accommodation

---

[13] (a) Sheldrick, G. M. *SHELXTL*, version 5.1; Bruker Analytical X-ray Instruments Inc.: Madison, WI, 1998. (b) Sheldrick, G. M. *SHELX-97*, PC version; University of Göttingen: Göttingen, Germany, 1997.

[14] (a) Agterberg, F. P. W.; Kluit, H. A. J. P.; Driessen, W. L.; Oevering, H.; Buijs, W.; Lakin, M. T.; Spek, A. L.; Reedijk, J. *Inorg. Chem.* **1997**, *36*, 4321 and references cited therein; (b) Zheng, Y. Z.; Tong, M. L.; Zhang, W. X.; Chen, X. M.; Grandjean, F.; Long, G. J. *Angew. Chem., Int. Ed.* **2007**, *46*, 6076. (c) Chen, P. K.; Che, Y. X.; Zheng, J. M.; Batten, S. R. *Chem. Mater.* **2007**, *19*, 2162.

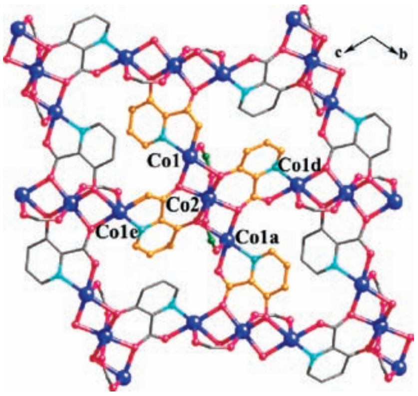

Figure 2. Plot of a 2D sheet showing the carboxylate bridges within and between the Co1−Co2−Co1a trimers in **1**.

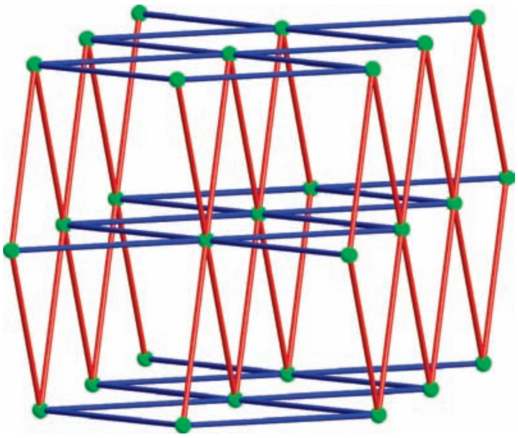

Figure 3. Schematic view of the bcc topology of **1**, in which each 8-connected Co_3 SBU (green ball) is extended by four pico (blue rods) and four pybz (red rods) ligands.

of the guest solvent molecules. Compared with our previous systems based on pico and other coligands (4,4′-bipyridine or isonicotinate), the μ_4-κN,O:κO′-μ_2:κO″-μ_2 binding fashion of pico in this case seems more interesting from a magnetic point of view because of the existence of shorter bridges, which will be responsible for the fascinating magnetic behaviors of **1** as discussed below.

To fully understand the network structure of **1**, the topological approach is applied to simplify such a 3D coordination framework. Apparently, the Co^{II} trimers could be regarded as the secondary building units (SBUs) in the construction of this network. In fact, these trimers can be linked by either the shorter pico ligands or the longer pybz ligands to form two types of 2D 4^4 layers, in which each pico or pybz serves as the 2-connected spacer to bridge two adjacent cobalt(II) trimers. The mutual cross-link of two such types of 2D sublayers results in the final 3D structure, in which each cobalt(II) trimer is connected to eight adjacent Co_3 units via four pico (blue rods in Figure 3) and four pybz (red rods in Figure 3) ligands with the vertex symbol of $(4.4.4.4.4.4.4.4.4.4.4.4.4_3.4_3.4_3.4_3.4_3.4_3.4_3.4_3.4_3.4_3.4_3.4_3.*.*.*.*)$. As a consequence, this framework can be reduced to a uninodal 8-connected body-centered-cubic **(bcu)** topology (or CsCl lattice; see Figure 3) with the Schläfli symbol of $(4^{24}.6^4)$,[15] which is, however, distorted because of the discrepancy of pico and pybz spacers. A very similar structural paradigm for such a network arrangement has recently been observed in a metal−organic framework with tetranuclear Co^{II} clusters as SBUs.[9]

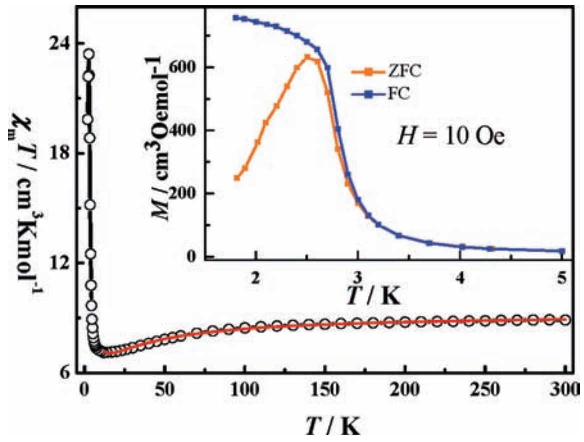

Figure 4. $\chi_m T$ vs T for **1**. The red solid line represents the best fit given in the text. Inset: ZFCM/FCM plots for **1** at low temperature.

Thermogravimetric analysis (TGA) was carried out to examine the thermal stability of compound **1** (Figure S3 in the Supporting Information). The crushed single-crystal sample was heated up to 850 °C in dinitrogen at a heating rate of 10 °C min^{-1}. The TGA curve for **1** shows that it is stable up to 440 °C without any weight loss, showing that the pillared-layer framework could retain structural integrity to ca. 440 °C. From 440 to 620 °C, there is a total loss of 74.0%, being consistent with pyrolysis of the coordinated organic ligands. The final residual weight is 26.1%, corresponding to CoO (calcd 26.5%). It can be concluded that **1** has a higher thermal stability compared with those commonly observed, which may be attributed to the presence of abundant coordination bonds of the pico ligand, pybz double bridges, the bridge-chelating effect of carboxylate groups, and the whole compact framework of **1**.[10a−d]

Magnetic Studies. The magnetic susceptibility per Co_3 unit measured on a polycrystalline sample of **1** under an applied field of 1000 Oe is shown in Figure 4. The $\chi_m T$ value at 300 K is 8.88 cm^3 mol^{-1} K, which is much higher than the spin-only value of 5.64 cm^3 mol^{-1} K for three spins with $S = {}^3/_2$ and $g = 2.00$,[1] owing to the significant orbital contribution of Co^{II} in an octahedral environment. Upon cooling, the $\chi_m T$ value decreases monotonically, reaching a minimum of 7.11 cm^3 mol^{-1} K at 12 K, then increases quickly to reach a maximum of 23.4 cm^3 mol^{-1} K at 2.6 K, and finally goes down to a minimum of 19.8 cm^3 mol^{-1} K at 2 K. The first decrease of $\chi_m T$ above 12 K should be due to the effect of spin−orbit coupling of the Co^{II} ion, resulting in an effective $S = {}^1/_2$ at low temperature from an $S = {}^3/_2$ at high temperature.[10,16] The quick increase of $\chi_m T$ between 2.6 and 12 K indicates ferromagnetic interactions or ferrimagnetic behavior

---

(15) (a) For interpretation of the three-letter net codes, see: Ockwig, N. W.; Delgado-Friedrichs, O.; O'Keeffe, M.; Yaghi, O. M. *Acc. Chem. Res.* **2005**, *38*, 176 and the associated website http://rcsr.anu.edu.au/. (b) Natarajan, S.; Mahata, P. *Chem. Soc. Rev.* **2009**, *38*, 2304.

(16) (a) Kambe, K.; Koide, S.; Usui, Y. *Prog. Theor. Phys.* **1952**, *7*, 15. (b) Sun, H. L.; Gao, S.; Ma, B. Q.; Su, G. *Inorg. Chem.* **2003**, *42*, 5399.

between the Co^{II} ions transported by μ_2-hydroxyl and/or μ_2-carboxylate oxygen bridges.[17,18] The reciprocal molar magnetic susceptibility plotted versus temperature obeys the Curie−Weiss law above 10 K with a Curie constant C = 8.89 cm^3 mol^{-1} K (Figure S3 in the Supporting Information) and a Weiss temperature $\theta = -2.51$ K. The negative θ is larger than the typical fitted θ value of ca. −14 K for the mononuclear cobalt(II) complexes[17a] and smaller than that for $(C_3H_4NSO_3)_2Co\cdot 4H_2O$ (ca. −0.92 K),[17b] where the Co^{II} ions have a CoN_2O_4 environment similar to that of **1**. The negative value of the Weiss temperature is likely related to the effect of spin−orbit coupling that stabilizes an effective spin doublet state, also indicating possible ferromagnetic interactions between the Co^{II} ions. In fact, it is rather difficult to really come to a conclusion about ferromagnetic couplings on the basis of the value of θ. For instance, a ferrimagnetic, or uncompensated antiferromagnetic state, would also lead to a lower absolute value of θ. In a fully ferromagnetic case, one would expect almost no minimum of χT. The θ value of cobalt networks depends on the exchange coupling but also reflects the single-ion spin−orbit coupling, which can vary with the ligand field.[10,17,18]

To investigate the magnetic behavior, where the $\chi_m T$ vs T curve rises abruptly at the low temperature for **1**, a noncritical scaling theory with the following simple phenomenological equation was used to fit the experimental data from 300 to 10 K:[19]

$$\chi_m T = A \exp(-E_1/kT) + B \exp(-E_2/kT)$$

Here, $A + B$ equals merely the high-temperature Curie constant and $E_1 > 0$ represents the "activation energy" corresponding to the spin−orbit coupling, which is responsible for the initial high-temperature decay of $\chi_m T$. The low-temperature behavior, increasing below 12 K, is denoted by the second term with $E_2 < 0$, which is ferromagnetic-like. The best fit gives $A + B = 9.1$ cm^3 K mol^{-1}, which is consistent with those obtained from the Curie−Weiss law in the high-temperature range ($C \approx 8.9$ cm^3 K mol^{-1}), and E_1/k = 32.7 K for the effect of spin−orbit coupling and site distortion (E_1/k on the order of +100 K)[1a] and E_2/k = 2 K found for more ferrimagnetic-like behavior rather than purely ferromagnetic exchange interaction.[10b,c] The fitting of **1** using the BKT model for T^{-1}−$\chi_m T$ cannot give in the 2.6−12 K temperature range a satisfactory fitting result. The value of **1** in the high-temperature range is 1.5 times that of the spin only; obviously, the spin−orbit coupling is strong, both of which give a reasonable estimate that this is not a XY system.[3d,9]

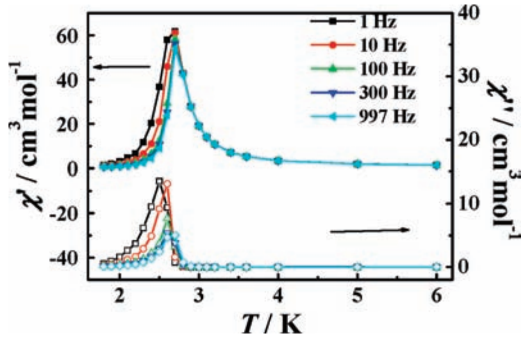

Figure 5. Temperature dependence of in-phase and out-of-phase ac magnetic susceptibility for **1** obtained at a zero external magnetic field.

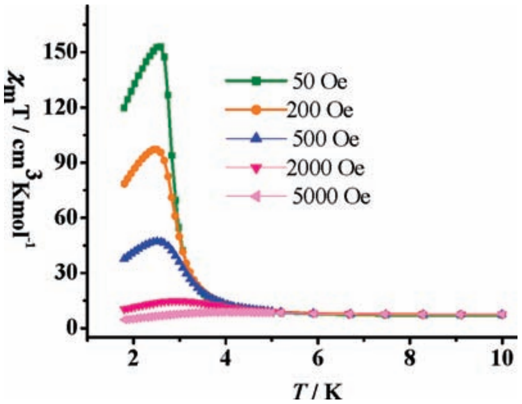

Figure 6. Temperature dependence of the susceptibility in different applied magnetic fields.

To gain more insight into the magnetic behavior at low temperature, zero-field-cooled/field-cooled magnetic (ZFCM/FCM) and alternating-current (*ac*) magnetic susceptibility measurements were performed for **1** (Figures 4 and 5). The ZFCM/FCM plots display irreversibility between the ZFCM/FCM curves below 2.6 K, indicating the onset of long-range magnetic ordering below 2.6 K (Figure 4). This is also evidenced by zero-field *ac* susceptibility measurement (Figure 5). With a decrease in the temperature, the out-of-phase part of the *ac* magnetic susceptibility shows no zero value below 3 K, from which T_c = 2.6 K was determined as the maximum of χ_m'. In addition, a slight frequency dependence of ac magnetic susceptibilities was found ($\Phi = \Delta T_p/[T_p \Delta(\log f)] = 0.009$), suggesting the presence of a degree of spin-glass behavior.[20] The temperature dependences of the susceptibilities in different applied magnetic fields (Figures 6 and S4 in the Supporting Information) are compatible with the ferrimagnetism.[10e] Below 3.5 K, χ_m rapidly increases and reaches their high maximum value at around 2.6 K before eventually falling at 2.0 K. The gradual decrease of χ_m in different higher applied magnetic fields is best ascribed to a saturation effect. The magnetic study of Co^{II} with the octahedral coordination environment reveals that it can show different magnetic anisotropies that are quite sensitive to the coordination environment. The electron spin resonance study of Co^{II} done by Gatteschi indicates that Co^{II} with

---

(17) (a) Wang, X. Y.; Li, B. L.; Zhu, X.; Gao, S. *Eur. J. Inorg. Chem.* **2005**, 3277. (b) Legrand, Y. M.; van der Lee, A.; Masquelez, N.; Rabu, P.; Barboiu, M. *Inorg. Chem.* **2007**, *46*, 9083. (c) Rabu, P.; Janvier, P.; Bujoli, B. *J. Mater. Chem.* **1999**, *9*, 1323.

(18) (a) Kurmoo, M. *Inorg. Chem.* **2003**, *42*, 5399. (b) Bauer, E. M.; Bellitto, C.; Righini, G.; Colapietro, M.; Portalone, G.; Drillon, M.; Rabu, P. *Inorg. Chem.* **2008**, *47*, 10945.

(19) (a) Miller, J. S.; Drillon, M. *Magnetism: Molecule to Materials V*; Willey-VCH: Weinheim, Germany, 2005; pp 347−377. (b) Rueff, J. M.; Paulsen, C.; Souletie, J.; Drillon, M.; Rabu, P. *Solid State Sci.* **2005**, *7*, 431. (c) Rueff, J. M.; Masciocchi, N.; Rabu, P.; Sironi, A.; Skoulios, A. *Chem.—Eur. J.* **2002**, *8*, 1813.

(20) Mydosh, J. A. *Spin Glass: an Experimental Introduction*; Taylor & Francis: London, 1993.

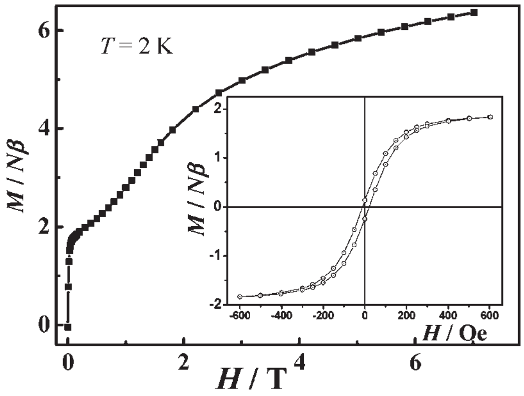

Figure 7. Field dependence of the magnetization at 2 K. Inset: hysteresis loop at 2 K.

elongated an octahedral coordination environment will show XY-type magnetic anisotropy.[21] While in the compressed octahedral environment, Co^{II} ions can show Ising anisotropy.[3d,22] In compound **1**, within the trimer unit, the axes of the coordination octahedron are not completely parallel, which suggests that the spin orientation is also not completely parallel. Also, this might be the reason why the magnetic measurement show some sign of spin canting. Although spin canting might occur, we think the ferrimagnetic coupling still dominates, which is supported by the fact that the maximum $\chi_m T$ values at low temperature are nearly 4 times larger than that at room temperature and, for canted antiferromagnetism, it is always smaller than the one at room temperature because of the well-known small canting angle.

Interestingly, the magnetization increases very fast from zero to ca. 1.5 μ_B at 0.03 kOe (Figure 7). After a slow increase to about 1.6 μ_B at 0.05 kOe, the magnetization increases faster again to 6.4 μ_B at 70 kOe. The saturation magnetization at 70 kOe approximates to 2.13 μ_B per cobalt, which is close to the expected value gS for $g = 4.3$ and $S = {}^{1}/_{2}$.[23] Therefore, it is reasonable to conclude that the moments of intratrimer Co atoms are aligned antiparallel. Zero-field splitting, and the more common complications arising from spin−orbit interactions, is a frequent source of difficulty in the interpretation of the magnetic data for Co^{II} complexes.[10] The magnitude of the coupling constants in the 3D network of **1** cannot be calculated by conventional methods. The reason for the step at low field in the magnetization versus field loop and a further increase at the higher field could be due to anisotropy stabilizing the uncompensated or nonlinear antiferromagnetic arrangement, with a spin flip for fields higher than 0.05 kOe, because of the weakened magnetic anisotropy of the Co^{II} ion, together with the complicated magnetic anisotropy of the 3D structure.[9,10f] However, the contribution of the diverse magnetic interactions with the slight changing of environments of the cobalt(II) centers, and the incompletely parallel situation of spin orientation, may play a role in this phenomenon.[5,19] Furthermore, a characteristic hysteresis loop is observed at 2 K with a remanent magnetization (M_r) of 0.18 μ_B and a coercive field (H_c) of 15 Oe (Figure 6, inset). Because a ferromagnetic long-range ordering would lead to full saturation and large remnant magnetization, the occurrence of the step at 2.13 μ_B and the weakness of M_r highly suggest that **1** is not a pure ferromagnet but rather a ferrimagnetic system.[5,10e]

Because of the longer interlayer Co···Co distance, compound **1** can be considered a 2D magnetic system and two kinds of magnetic interactions can be considered, i.e., intratrimer and intertrimer within the layer. Within each trimer, there are three sets of magnetic exchange pathways: μ_2-hydroxyl and μ_2-carboxylate oxygen atoms of pico and *syn,syn*-carboxylate of pybz, cooperatively contributed by the antiferromagnetic coupling transported by mixed bridges.[10b−f,23,24] In addition, the intertrimer magnetic interactions through bichelated pico bridges, mainly the 1,1,3-μ_3-carboxylate configuration within the layer, also feature a weakly ferromagnetic coupling[8] and result in the final 2D ferrimagnetic layer. These magnetic interactions, together with the anisotropy of the Co^{II} ions, favor a ferrimagnetic long-range ordering below 2.6 K and a spin−flip transition. An appropriate balance between the crystallographic symmetry, the anisotropy, the nearest interactions, and the next-nearest interactions is needed to observe these interesting magnetic phenomena.[10f] Well-isolated layer structures in the metal−organic framework family are very rare. The long-range magnetic ordering is induced by the dipolar interaction between layers of highly correlated moments.[5,25] However, the weak interlayer exchange interactions can be easily overcome under application of a magnetic field. For example, a linear trimer-based Co^{II} compound pillared by isonicotinate ligands is a normal metamagnet with a low critical field.[10b] In the present case, the interlayer interactions (Co···Co distance of ca. 12.4 Å) are either negligible or weakly ferromagnetic, and then the magnetism is probably restricted to two dimensions only.[25]

Conclusion

In summary, this work shows the construction of a layer-based homospin ferrimagnet by using mixed magnetic exchange pathways of μ_2-hydroxyl, μ_2-carboxylate oxygen and 1,1,3-μ_3-carboxylate bridges, featuring a pillared-layer motif with **bcu** topology. The present results further demonstrate, in line with previous studies, that 3-hydroxypicolinate has the potential to generate novel coordination frameworks with promising structural features and magnetic properties.

---

(21) Bencini, A.; Benelli, C.; Gatteschi, D.; Zanchini, C. *Inorg. Chem.* **1980**, *19*, 1301.

(22) Lescouzec, R.; Vaissermann, J.; Ruiz-Perez, C.; Lloret, F.; Carrasco, R.; Julve, M.; Verdaguer, M.; Dromzee, Y.; Gatteschi, D.; Wernsdorfer, W. *Angew. Chem., Int. Ed.* **2003**, *42*, 1483.

(23) (a) Zeng, M. H.; Yao, M. X.; Liang, H.; Zhang, W. X.; Chen, X. M. *Angew. Chem., Int. Ed.* **2007**, *46*, 1832. (b) Goodenough, J. B. *Magnetism and the Chemical Bond*; Interscience: New York, 1963.

(24) (a) Feyerherm, R.; Rabu, A.; Loosea, P.; Drillon, M. *Solid State Sci.* **2003**, *5*, 321. (b) Livage, C.; Egger, C.; Férey, G. *Chem. Mater.* **1999**, *11*, 1546. (c) Huang, Z. L.; Drillon, M.; Masciocchi, N.; Sironi, A.; Zhao, J. T.; Rabu, P.; Panissod, P. *Chem. Mater.* **2000**, *12*, 2805. (d) Kumagai, H.; Kepert, C. J.; Kurmoo, M. *Inorg. Chem.* **2002**, *41*, 3410. (e) Angelov, S.; Drillon, M.; Zhecheva, E.; Stoyanova, R.; Belaiche, M.; Derory, A.; Herr, A. *Inorg. Chem.* **1992**, *31*, 1514.

(25) (a) Kurmoo, M. *Chem. Mater.* **1999**, *11*, 3370. (b) Zhang, Y. Y.; Zeng, M. H.; Qi, Y.; Sang, S. Y.; Liu, Z. M. *Inorg. Chem. Commun.* **2007**, *10*, 33. (c) Delahaye, É.; Eyele-Mezui, S.; Bardeau, J.; Leuvrey, C.; Mager, L.; Rabu, P.; Rogez, G. *J. Mater. Chem.* **2009**, *19*, 6106. (d) Demessence, A.; Rogez, G.; Rabu, P. *Chem. Mater.* **2006**, *18*, 3005.

Acknowledgment. This work was supported by the NSFC (Grants 20871034 and 20801006), GXSFC (Grant 0832001Z), Program for New Century Excellent Talents in University of the Ministry of Education China (Grant NCET-07-217), and Project of Ten, Hundred, Thousand Distinguished Talents in New Century of Guangxi (Grant 2006201) as well as Fok Ying Tung Education Foundation (Grant 111014).

Supporting Information Available: X-ray crystallographic data in CIF format, temperature dependence plots, FT-IR spectroscopy, and a TGA curve. This material is available free of charge via the Internet at http://pubs.acs.org.